




ARTICLE

LHX2 haploinsufficiency causes a variable neurodevelopmental disorder



Cosima M. Schmid^{1,2}, Anne Gregor^{1,2,3}, Gregory Costain^{4,5,6}, Chantal F. Morel^{7,8}, Lauren Massingham⁹, Jennifer Schwab⁹, Chloé Quélin¹⁰, Marie Faucher^{11,12}, Julie Kaplan¹³, Rebecca Procopio¹³, Carol J. Saunders^{14,15}, Ana S.A. Cohen^{14,15}, Gabrielle Lemire^{16,17}, Stephanie Sacharow¹⁷, Anne O'Donnell-Luria^{16,17}, Ranit Jaron Segal¹⁸, Jessica Kianmahd Shamshoni¹⁹, Daniela Schweitzer¹⁹, Darius Ebrahimi-Fakhari²⁰, Kristin Monaghan²¹, Timothy Blake Palculict²¹, Melanie P. Napier²¹, Alice Tao²², Bertrand Isidor²³, Kamran Moradkhani²³, André Reis^{24,25}, Heinrich Sticht²⁶, Care4Rare Canada²⁷, Wendy K. Chung²⁸, Christiane Zweier^{1,2,3,*} 

ARTICLE INFO

Article history:

Received 16 November 2022

Received in revised form

3 April 2023

Accepted 5 April 2023

Available online 11 April 2023

Keywords:

ASD

Intellectual disability

LHX2

Microcephaly

NDD

Neurodevelopmental disorder

ABSTRACT

Purpose: *LHX2* encodes the LIM homeobox 2 transcription factor (*LHX2*), which is highly expressed in brain and well conserved across species, but it has not been clearly linked to neurodevelopmental disorders (NDDs) to date.

Methods: Through international collaboration, we identified 19 individuals from 18 families with variable neurodevelopmental phenotypes, carrying a small chromosomal deletion, likely gene-disrupting or missense variants in *LHX2*. Functional consequences of missense variants were investigated in cellular systems.

Results: Affected individuals presented with developmental and/or behavioral abnormalities, autism spectrum disorder, variable intellectual disability, and microcephaly. We observed nucleolar accumulation for 2 missense variants located within the DNA-binding HOX domain, impaired interaction with co-factor LDB1 for another variant located in the protein-protein interaction–mediating LIM domain, and impaired transcriptional activation by luciferase assay for 4 missense variants.

Conclusion: We implicate *LHX2* haploinsufficiency by deletion and likely gene-disrupting variants as causative for a variable NDD. Our findings suggest a loss-of-function mechanism also for likely pathogenic *LHX2* missense variants. Together, our observations underscore the importance of *LHX2* in the nervous system and for variable neurodevelopmental phenotypes.

© 2023 American College of Medical Genetics and Genomics.

Published by Elsevier Inc. All rights reserved.

Cosima M. Schmid and Anne Gregor contributed equally.

Wendy K. Chung and Christiane Zweier contributed equally.

*Correspondence and requests for materials should be addressed to Christiane Zweier, Department of Human Genetics, Inselspital Bern, University of Bern, Freiburgstrasse 15, 3010 Bern, Switzerland. *Email address:* Christiane.zweier@insel.ch

Affiliations are at the end of the document.

doi: <https://doi.org/10.1016/j.gim.2023.100839>

1098-3600/© 2023 American College of Medical Genetics and Genomics. Published by Elsevier Inc. All rights reserved.

Introduction

Neurodevelopmental disorders (NDDs) are clinically and genetically extremely heterogeneous, with defects in more than 1500 genes implicated to date (SysNDD database¹). Many NDD genes/proteins are connected in molecularly and functionally coherent modules, one of them being transcriptional regulation.¹ A key transcriptional regulator is the well-conserved LIM homeobox 2 transcription factor, encoded by *LHX2*.² *LHX2* is known to bind to enhancers of numerous important developmental genes³ and is involved in regulating chromatin accessibility in various developmental processes.^{4,5} As part of the LIM gene family, *LHX2* contains 2 tandem cysteine-rich LIM domains, binding to zinc, and a homeobox domain.⁶ With the zinc-binding LIM domains, *LHX2* can form multimeric complexes,⁷ for example, with the ubiquitously expressed co-factor LDB1 in mammals.⁸ As an active tetramer, it then binds to DNA via the HOX domain to activate target genes.⁹ *LHX2* is particularly relevant in early embryonic development, in which its role in brain, eye, and erythrocyte development was illustrated by in utero lethality of *LHX2*^{-/-} mice.¹⁰ Additionally, several murine models have revealed that *LHX2* is centrally involved in hair follicle development,¹¹ olfactory receptor organization,⁵ and liver regeneration.¹² *LHX2* has also been shown to be important for proper spatial forebrain and hippocampal development,¹³ as well as the formation of the corpus callosum.¹⁴ Variants in *LHX2* have not been previously linked to any genetic disorder in OMIM.

Through international collaboration, we identified mostly de novo deletions, likely gene-disrupting (LGD) or missense variants in *LHX2* in 19 individuals from 18 families presenting with a variable neurodevelopmental phenotype with global developmental delay, intellectual disability, microcephaly, autism spectrum disorder, and other behavioral anomalies. Alterations in subcellular localization, impaired protein-protein interaction, or impaired transcriptional activation indicate a loss-of-function effect, as postulated for LGD variants, also for missense variants.

Materials and Methods

Ascertainment of affected individuals

After identification of a de novo LGD *LHX2* variant in 1 individual by trio-exome sequencing, clinical and genetic variant details of 18 additional individuals from 17 families with variants in *LHX2* were assembled using GeneMatcher,¹⁵ the literature, and through personal communication. Genetic testing in various centers was performed either in a clinical diagnostic setting (I1, I3-6, I8-I10, I13-I18) or in a research setting (I2, I7, I11, I12, I19)

approved by the ethical review board of the respective collaborating institutions (Supplemental Table 1). The deletion in I1 was identified through chromosomal microarray analysis, and the variants in I2-I19 were identified through exome sequencing (either singleton, duo, or trio exome, as listed in Supplemental Table 1). For publication of genetic and clinical data (as well as publication of affected individuals' photographs), informed consent was obtained from the individuals, their parents, or legal guardians. For description of *LHX2* variants, reference sequences NM_004789.4 and NP_004780.3 were used.

Structural modeling

The *LHX2* LIM domains in complex with LDB1 were modeled using the crystal structure of the ISL1-LDB1 complex as a template (PDB code: 4JCJ¹⁶). The *LHX2* HOX domain in complex with DNA was modeled using the Homeobox protein aristaless in complex with DNA as a template (PDB code: 3A01¹⁷). Modeling of the variants was performed with SwissModel,¹⁸ and RasMol¹⁹ was used for structure analysis and visualization.

Immunofluorescence

Immunofluorescence was performed in HeLa cells. HeLa cells were grown on coverslips and transfected with Myc-tagged wild-type or mutant *LHX2* using the jetPrime (Polyplus-transfection) system according to manufacturer's instructions. Cells were fixated 48 hours after transfection in 4% paraformaldehyde in phosphate-buffered saline for 10 minutes at room temperature. Staining was performed with antibodies against anti-c-Myc (M4439, Sigma-Aldrich), GAPDH (2188, Cell Signaling) and Nucleolin (14574, Cell Signaling). Secondary antibodies used were Alexa Fluor 488 goat anti-mouse (A11001, Thermo Scientific) and Alexa Fluor 546 donkey anti-rabbit (A10040, Thermo Scientific). Nuclei were counterstained with DAPI (Serva). Images were taken with a Zeiss Axio Imager Z2 Apotome microscope (Zeiss) with a 63× objective and analyzed in ImageJ. For quantification of the aggregation phenotype, 100 cells were analyzed for each variant tested. Aggregates were defined as visually identified accumulations of *LHX2* that were sharply set apart from the background measuring at least 2 μm. Cells were counted as aggregate positive if they contained at least one of these *LHX2* aggregates. Significance was calculated using a Fisher exact test.

Sodium dodecyl sulfate–polyacrylamide gel electrophoresis and western blot

Sodium dodecyl sulfate (SDS)–polyacrylamide gel electrophoresis (PAGE) and western blotting are described in the Supplemental Methods in more detail.

Co-immunoprecipitation

For protein-protein interaction analysis of LHX2 and the known interaction partner LDB1, HEK293 cells were transfected with Myc-tagged wild-type or mutant *LHX2* and Flag-tagged *LDB1* or their respective negative controls using the jetPrime system. After cell lysis with RIPA lysis buffer (50 mM Tris pH 8.0, 150 mM NaCl, 1% Igepal CA-630, 0.1% SDS, 0.5% sodium-deoxycholate) with 1/100 protease inhibitor, samples were incubated with Protein A Mag Sepharose bead suspension (GE Healthcare) and anti-myc (M4439, Sigma-Aldrich) antibody at 4 °C overnight. Subsequently, beads were washed in RIPA lysis buffer, and TBS and samples were eluted with 1× Laemmli buffer. SDS-PAGE and western blotting were performed as described above. For quantification from 3 independent replicates, bands for FLAG-tagged LDB1 IP and Myc-tagged LHX2 IP were each normalized to their respective inputs. The ratio of both normalizations was used for quantification. Significance was calculated using a one-sample *t* test with theoretical value set to 1. Co-IP for MSX1 (FLAG) and LSD1 (FLAG) was performed as described above.

Luciferase assay

To test transcriptional activation ability of wild-type and mutant LHX2, a dual-luciferase assay was conducted using the pGL3 vector (Promega) in a neuroblastoma cell line, SK-N-BE(2). LHX2 was found to show transactivation activity already on the empty pGL3 vector, as has been reported for several other genes before.²⁰ This activation is likely due to cryptic enhancer sites within the pGL3 that are bound by LHX2. Addition of known LHX2 responsive elements (eg, CER1 enhancer and promoter,³ GFAP promoter, and TSHB promoter) to the pGL3 vector did not result in increased or decreased transactivation (data not shown). We also tested these constructs in different cell lines (hiPSC, HEK293, HeLa, Jeg3, and SK-N-BE(2)) and failed to see activation beyond activation of the empty pGL3 vector, which was strongest in SK-N-BE(2) cells. For the assay, SK-N-BE(2) cells were transiently transfected using the jetPrime system (Polyplus-transfection) with wild-type or mutant *LHX2* constructs and the pGL3 vector (Promega) or their negative controls, respectively. To normalize for differences in transfection efficiency, a renilla luciferase vector was co-transfected. Preparation of samples and luminescence measurements were performed with the Dual-Luciferase Kit (Promega) according to manufacturer's instructions. Luminescence was measured on a SpectraMax iD3 Luminometer (Molecular Devices). Analysis was performed in 3 independent experiments, and each experiment was performed in triplicate. *P* values were calculated using the *t* test.

Results

Variant spectrum encompasses LGD and missense variants

We assembled 1 small chromosomal deletion, 10 LGD, and 7 missense variants in *LHX2* (Figure 1A, Supplemental Figure 1, Supplemental Table 1). Five of the variants were previously included in large studies on de novo variants in developmental disorders or congenital heart disorders, but without detailed clinical information,^{21,22} and 3 variants are from the SPARK autism cohort²³ (Supplemental Table 1). Thirteen of the variants were de novo; for 5 cases, parental samples were not available, and 1 variant (p.(Arg318Leu)) was inherited from a mildly affected mother (I15 and I16).

The chromosomal deletion encompasses the complete *LHX2* coding sequence and the first exon of *DENNDIA*. Seven of the LGD variants are located upstream of the last exon and are likely to lead to nonsense-mediated messenger RNA decay (NMD). Three variants are located in the ultimate exon and may therefore escape NMD. Two of them (p.(Trp313Ter) and p.(Leu326PhefsTer41)) localize to the DNA-binding HOX domain, and the third (p.(Gly332AlafsTer45)) resides downstream of any annotated domain. For the 2 variants located in the HOX domain, we confirmed expression of truncated LHX2 protein by western blot (Supplemental Figure 2A), indicating that these variants may lead to stable expression of shortened proteins lacking part of the HOX domain and more than one-fifth of the original protein sequence, if escaping NMD. Two of the 7 missense variants are located in one of the 2 LIM domains each (LIM1: p.(Cys80Ser) and LIM2: p.(Cys146Tyr)), and 3 reside in the HOX domain (p.(Lys294Glu), p.(Asn316-Lys), and p.(Arg318Leu)). All 5 identified missense variants located to annotated domains are predicted to be pathogenic by at least 3 prediction programs (Supplemental Table 2). None of them were reported in the Genome Aggregation Database (gnomAD).²⁴ All but 1 missense variant affect highly conserved amino acid positions, whereas position 207 (p.(Asn207Lys)) is not conserved in zebrafish or *Drosophila melanogaster* (Supplemental Figure 1). For the variants p.(Asn207Lys) and p.(Asn215Ser), not localizing to any of the annotated functional domains, another missense variant affecting the same residue was found in gnomAD once. The relevance of the 2 missense variants outside of annotated domains remains currently unclear. After functional testing of several missense variants (see section "Altered transactivation activity of *LHX2* missense variants", Supplemental Table 3), we also consider the relevance of p.(Lys294Glu) to be unclear. Of note, 1 individual (I13) also carries a likely pathogenic variant in *RUNX2*, associated with cleidocranial dysplasia (MIM 119600), which may explain his short stature and his skeletal anomalies (Supplemental Table 1). Another individual

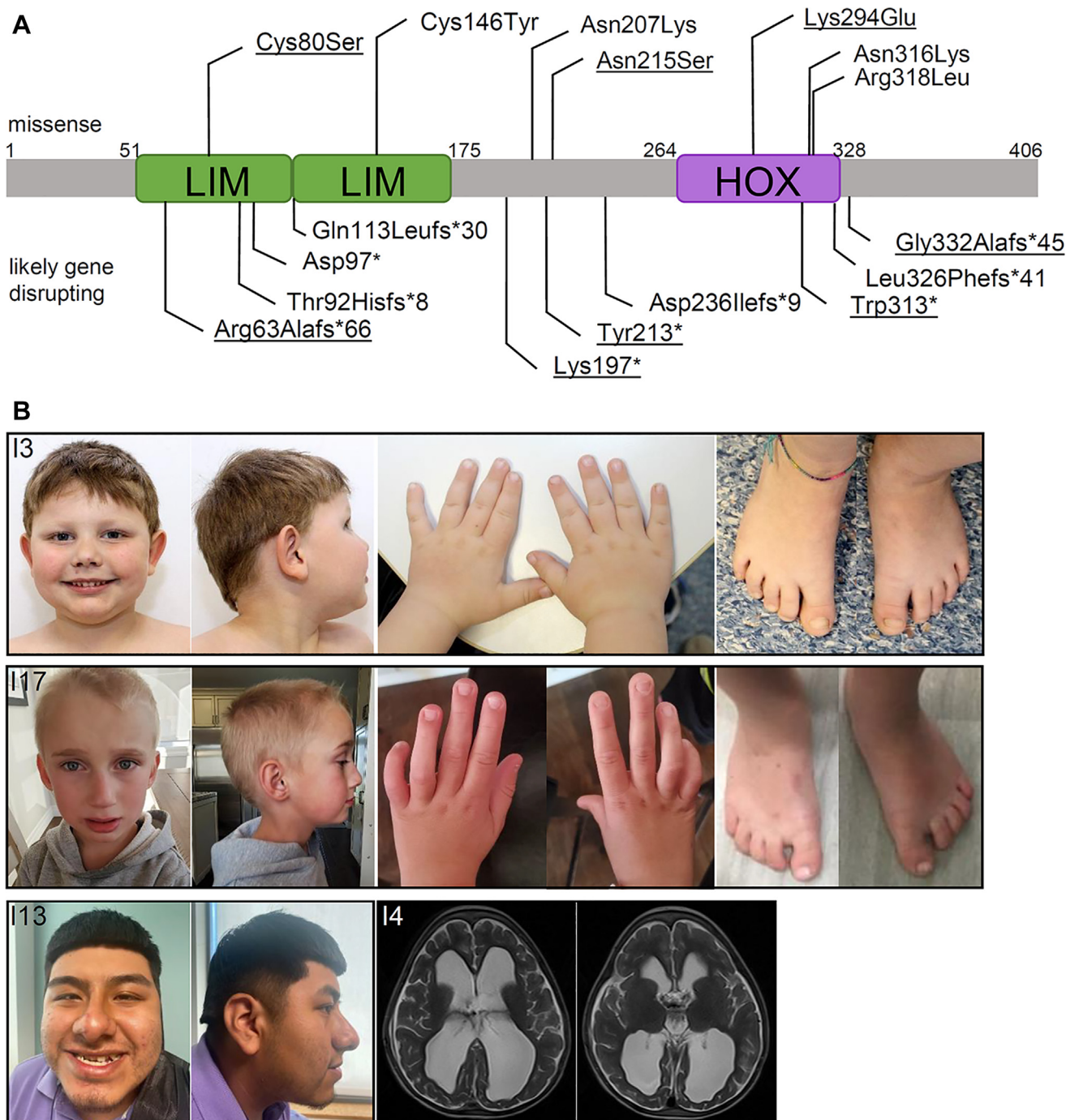


Figure 1 *LHX2* variants identified in individuals with NDDs. A. Schematic drawing of the protein structure of *LHX2* (NM_004789.4, NP_004780.3) with identified variants. Missense variants are displayed above the scheme, likely gene-disrupting variants below. Not displayed here is an additional chromosomal deletion, which affects the complete *LHX2* gene (I1). Eight variants previously published are underlined.²¹⁻²³ Domains are color coded according to InterPro. B. Clinical images with pictures of frontal and lateral face (I3, I13, I17) and hands and feet (I3, I17). Note minor unspecific facial dysmorphism in all individuals and short fingernails and toenails in individuals I3 and I17. Magnetic resonance imaging of axial T2 of I4 showing diffuse white matter loss and ventriculomegaly.

(I18) carries an additional de novo variant in another candidate disease gene (*PSMA7*), which may possibly contribute to her phenotype. According to gnomAD²⁵

constraint scores, *LHX2* is highly intolerant of LoF variants ($PII = 0.99$, observed/expected = 0, $LOEUF = 0.22$) and carries fewer missense variants than expected

(Z score = 2.27, observed/expected = 0.59 [0.51-0.68]). Variants are described based on reference NP_004780.3.

Variable clinical spectrum associated with *LHX2* variants

For description of the clinical phenotype, we did not include the 3 affected individuals with missense variants whose relevance we consider uncertain at the moment (I17-I19) and instead focused on the 16 individuals with a deletion, LGD variants, or missense variants, which we consider (likely) pathogenic. Most affected individuals with variants for whom detailed clinical data were available showed variable degrees of intellectual disability (ID), developmental delay, and/or autism spectrum disorder (ASD) (14 of 16). Behavioral anomalies were commonly described (10 individuals), including attention deficit, hyperactivity, aggressive and self-injurious behavior, as well as autism spectrum disorders. Delay in speech development was reported in 10 individuals, with variably impaired speech abilities, ranging from being nonverbal to mild speech impediments. Five individuals had sleeping difficulties. Magnetic resonance imaging anomalies included dysgenesis of the corpus callosum, enlarged ventricles, and white matter lesions and were relatively frequent (5 of 7) (Figure 1B). Hypotonia was noted in 3 individuals, and febrile seizures occurred in 1 individual. Seven of 10 individuals were noted to be microcephalic postnatally (z scores of -2.6 to -4.1), and 1 was macrocephalic (z score 3.6). Short stature was observed in 3 individuals (z scores of -2.1 to -3.4). Ophthalmologic abnormalities were common (9 of 13), including macular degeneration, optic neuropathy, and esotropia. Variable and infrequent other abnormalities, such as feeding difficulties, congenital heart disease, or minor skeletal anomalies, were observed in 2 to 3 individuals each. Subtle facial dysmorphisms were noted in most of the individuals but were nonspecific without a recognizable facial gestalt (Figure 1B). No obvious differences in clinical phenotypes regarding LGD or missense variants were noted (Table 1). Detailed clinical information on the individuals with clear variants summarized here and additionally individuals with uncertain variants is provided in Supplemental Table 1.

Structural modeling of *LHX2* missense variants

The cysteines affected by variants p.(Cys80Ser) and p.(Cys146Tyr) are located in the first and second LIM domains, respectively (Figure 2A). Both cysteines are highly conserved in LIM domains because they are involved in zinc ion binding. A replacement of cysteine by serine or tyrosine is predicted to result in a loss of the zinc ion, thereby disturbing the domain structure. The first and second LIM domains are both involved in LDB1 binding (Figure 2A). Unfolding of one of the LIM domains by the

Table 1 Clinical data summary of likely pathogenic variants

Variant Type	Likely Gene		
	Disrupting ($n = 11$)	Missense ($n = 5$)	All ($N = 16$)
ID/DD/ASD	9/11	5/5	14/16
Behavioral anomalies (including ASD)	6/8	4/4	10/12
Speech impairment	6/7	4/4	10/11
Seizures/abnormal EEG	1/5	0/3	1/8
Hypotonia	2/6	1/3	3/9
Facial dysmorphism	6/7	3/3	9/10
Microcephaly	4/7	3/3	7/10
Macrocephaly	1/7	0/4	1/10
Feeding difficulties	2/5	0/3	2/8
Sleeping difficulties	3/5	2/4	5/9
Vision impairment	6/9	3/4	9/13
MRI anomalies	4/5	1/2	5/7
Cardiac defects	3/8	0/3	3/11
Skeletal anomalies	2/8	1/3	3/11

Only cases with likely disease-causing variants are included (I1 – I16); numbers take into account individuals displaying specific symptoms/individuals with phenotypic information available for this symptom.

ASD, autism spectrum disorder; DD, developmental delay; EEG, electroencephalography; ID, intellectual disability; MRI, magnetic resonance imaging.

variant is therefore expected to decrease binding affinity for LDB1.

The variants p.(Lys294Glu), p.(Asn316Lys), and p.(Arg318Leu) are located in the DNA-binding HOX domain (Figure 2B). A closer inspection of the structure reveals that Asn316 and Arg318 form tight polar interactions with the DNA (Figure 2C), which play an important role for the specificity and affinity of complex formation. These interactions are lost in the p.(Asn316Lys) and p.(Arg318Leu) variants (Figure 2D and E), which is expected to severely impair DNA binding.

In contrast, p.(Lys294Glu) is not directly involved in DNA binding (Figure 2B). In homologous HOX domains, the respective sequence position was reported to interact with a second HOX domain, thereby causing cooperative DNA binding.¹⁷ Such a mechanism might also be feasible for LDB1 but cannot be further addressed by molecular modeling because of the lack of structural information.

The remaining 2 variants, p.(Asn207Lys) and p.(Asn215Ser), are located in a protein region for which no three-dimensional structural information exists. According to the predictions, this region is nonglobular and does not adopt a defined domain structure.

Altered localization of *LHX2* missense variants

To evaluate effects of *LHX2* missense variants, we performed in vitro assays for 6 of the 7 missense variants. Analysis of protein expression levels upon overexpression of wild-type-type and/or mutant Myc-tagged *LHX2* in

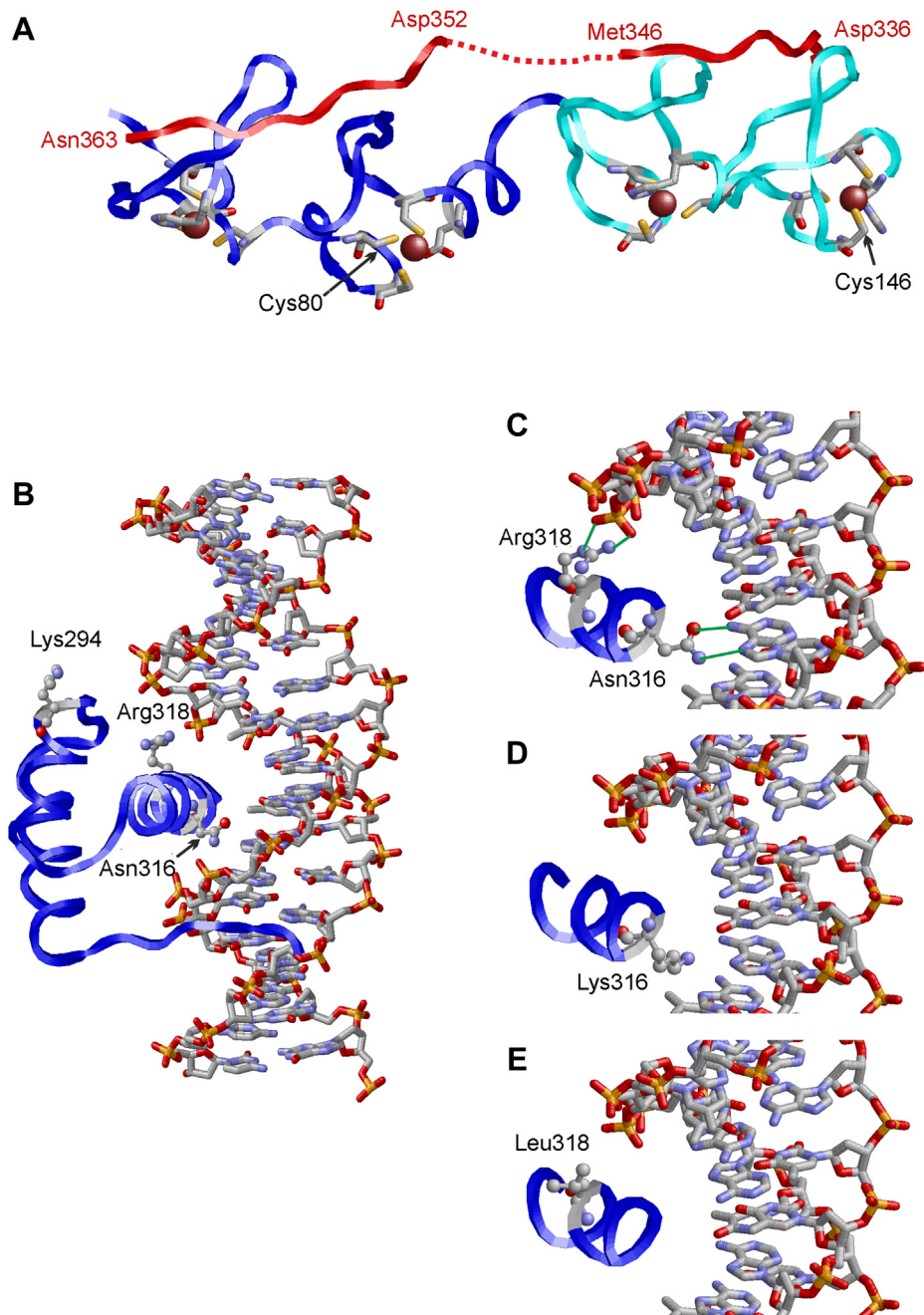


Figure 2 Structural modeling of LHX2. A. Structure of the LIM domain pair in complex with LDB1 (LIM1 in blue; LIM2 in cyan, LDB1 in red). Residues involved in the coordination of zinc ions are shown in stick presentation and those cysteines affected by the variants (Cys80, Cys146) are labeled (zinc ions shown as brown balls). LDB1 exhibits a bipartite interaction site (residues Asp336-Met346 and Asp352-Asn363) and binds both to the LIM1 and the LIM2 domain. B. Structure of the HOX domain (blue ribbon) in complex with DNA (stick presentation). Residues affected by the variants are shown in ball-and-stick presentation and are labeled. C. Enlargement of the binding site showing the interactions of Asn316 and Arg318 in detail. Asn316 and Arg318 form polar interactions (green lines) to an adenosine ring and a phosphoryl group, respectively. D. In the Asn316Lys variant, the longer lysine sidechain adopts a different orientation, leading to the loss of interactions with the adenosine ring. E. In the Arg318Leu variant, the nonpolar leucine sidechain cannot form the polar interactions with the phosphoryl group observed in the wild type.

HEK293 cells showed that LHX2 expression levels are unaffected by the tested missense variants regardless of whether missense variants are expressed alone or together with wild-type LHX2 (Supplemental Figure 2B-E).

Immunofluorescence after transfection of HeLa cells with constructs containing 6 of the missense variants confirmed nuclear localization of wild-type LHX2 with slightly stronger signal toward the perimeter of the nucleus

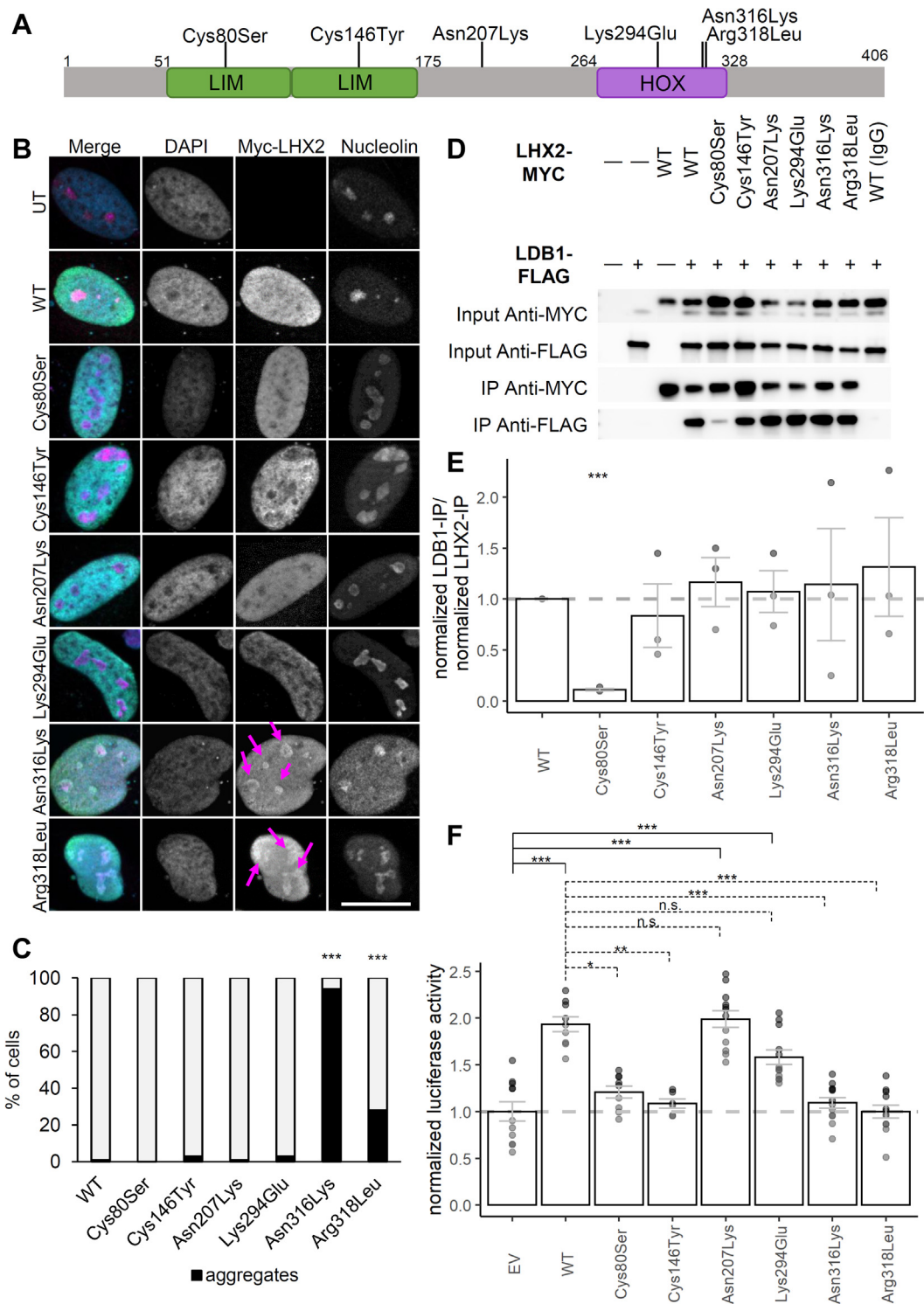


Figure 3 *LHX2* missense variants impair subcellular localization and protein-protein interaction. **A.** Schematic overview of localization of tested missense variants. **B.** Immunofluorescence on HeLa cells transiently transfected with Myc-tagged WT or mutant *LHX2* and costained with anti-Myc (green) and anti-Nucleolin (magenta) antibodies showed nuclear localization for the WT and all tested variants. Variants p.(Asn316Lys) and p.(Arg318Leu) resulted in formation of aggregates (magenta arrows), which mostly colocalize with nucleolin. Scale bar depicts 20 μ m. **C.** We quantified the formation of nuclear aggregates for WT *LHX2* and all 3 variants localized to the HOX domain (p.(Lys294Glu), p.(Asn316Lys), and p.(Arg318Leu)) for 100 cells per condition. Two of the variants (p.(Asn316Lys) and p.(Arg318Leu)) showed a significant increase in aggregate formation. *P* values were obtained using a Fisher exact test, ****P* < .001. **D.** Coimmunoprecipitation of Myc-tagged WT or mutant *LHX2* and Flag-tagged LDB1 or their respective negative controls showed reduced co-precipitation for a variant in the LIM domain (p.(Cys80Ser)). Co-immunoprecipitation was performed with an antibody against Myc and IgG as a negative

compared with the center (Figure 3B, Supplemental Figures 3 and 4). Four of the mutants behaved similar to the wild type, whereas 2 missense variants located in the HOX domain (p.(Asn316Lys) and p.(Arg318Leu)) resulted in formation of aggregates within the nucleus that were present in 94% and 28% of cells, respectively (Figure 3B and C, Supplemental Figures 3 and 4, Supplemental Table 3). The number of aggregates per cell ranged from 1 to 5. By co-staining with nucleolar marker nucleolin, most of these aggregates were confirmed to be in the nucleolus (Figure 3B, Supplemental Figure 4). Nucleoli were comparable between untransfected cells and cells overexpressing LHX2, suggesting that overexpression per se does not affect morphology of nucleoli (Figure 3B, Supplemental Figure 4). Computational predictions suggest that nuclear import of LHX2 still works for these 2 variants; however, DNA binding is predicted to be hampered (Figure 2D and E). This would be in line with the observed nucleolar aggregates.

A missense variant in the LIM domain impairs binding of LHX2 to LBD1

LHX2 is known to interact with LDB1 to form heterotetramers.⁸ To analyze whether the ability of LHX2 to bind LDB1 is impaired by the 6 tested missense variants, we performed a co-immunoprecipitation assay. Mutant LHX2, carrying the missense variant p.(Cys80Ser), localizing to the first protein-binding LIM domain, showed a reduced binding ability to LDB1. The missense variant located in the second LIM domain, p.(Cys146Tyr), and the other 4 tested missense variants resulted in similar binding abilities to the wild type (Figure 3D and E, Supplemental Figure 5, Supplemental Table 3). This binding behavior did not change when mixing mutant LHX2 equimolarly with wild-type LHX2, although more LDB1 could be bound likely due to the presence WT LHX2 (Supplemental Figure 6). Physical interaction with MSX1 or the NuRD complex subunit LSD1 is not impaired by any of the tested missense variants (Supplemental Figure 7).

Altered transactivation activity of LHX2 missense variants

To evaluate effects of missense variants on the ability of LHX2 to induce transcriptional activation, we performed a dual luciferase assay. We found impaired transactivation for both missense variants located in the LIM domains (p.(Cys80Ser) and p.(Cys146Tyr)) and the 2 missense variants located in the HOX domain that were predicted to impair DNA binding directly and were shown to aggregate in the nucleolus (p.(Asn316Lys) and p.(Arg318Leu)) (Figure 3F, Supplemental Table 3). The third missense variant located in the HOX domain and not predicted to impair DNA binding directly (p.(Lys294Glu) as well as the variant located outside of annotated domains (p.(Asn207-Lys)) showed no impairment of transactivation capabilities and similar luciferase activity levels as wild-type LHX2 (Figure 3F, Supplemental Table 3).

Discussion

Although a few variants were described in a large study on developmental disorders²¹ or in an autism cohort,²³ LHX2 defects have previously not been established as a cause of NDDs. By assembling variant and clinical data on 16 individuals with neurodevelopmental phenotypes and mostly de novo likely pathogenic variants in LHX2, we now identify it as an NDD-associated gene.

The LHX2-related neurodevelopmental phenotype is nonspecific and includes variable intellectual disability; speech impairment; autism spectrum disorder; behavioral, sleep, and brain magnetic resonance imaging abnormalities; and microcephaly. Additionally, nonspecific minor facial dysmorphism are observed. Although detailed clinical information was not available for all cases (including several of the previously reported individuals), the available detailed clinical information shows that the phenotypic spectrum associated with LHX2 defects is highly variable.

control. A representative image is shown, and the experiment was repeated 3 times. Uncropped blots can be found in Supplemental Figure 5. E. Quantification of co-immunoprecipitation from 3 independent replicates showed significantly reduced LDB1 co-precipitation for variant p.(Cys80Ser). Binding for all other variants was not altered. For quantification, LDB1 and LHX2 IP bands were normalized to their respective inputs, and then the ratio of normalized LDB1-IP to normalized LHX2-IP was calculated. Averages from all experiments are shown with standard deviation. Significance was calculated using a one-sample *t* test with theoretical value set to 1, ****P* < .001. F. WT LHX2 showed increased transcriptional activation in a dual-luciferase assay compared with the EV. Four of the 6 tested missense variants (p.(Cys80Ser), p.(Cys146Tyr), p.(Asn316Lys), and p.(Arg318Leu)) showed impaired transcriptional activation. For 2 variants (p.(Asn207Lys) and p.(Lys294Glu)), transcriptional activity was comparable to WT levels. As a reporter construct the pGL3 vector was used, which already showed specific transactivation, possibly due to cryptic enhancer sites as has been shown for other genes.²⁰ SK-N-BE(2) cells were transiently co-transfected with pGL3 reporter plasmid, an empty pcDNA3.1-Myc vector, WT or mutant LHX2, and a Renilla luciferase vector as a normalization control. Experiments were performed in triplicates and repeated independently 3 times. Averages from all experiments are shown with standard deviation. *P* values were obtained using a *t* test, **P* < .05, ***P* < .01, ****P* < .001. EV, empty vector; n.s., not significant; UT, untransfected cell; WT, wild-type.

Furthermore, the phenotypes observed in individuals with LGD and missense variants are comparable, and no genotype-phenotype correlations could be delineated. Additionally, no correlations between predicted or tested functional effects of variants and associated clinical phenotypes can be found, as, for example, the mildest and most severely affected cases carry frameshift variants likely to lead to a complete loss of 1 allele. Phenotypes associated with missense variants fall well within the phenotypic spectrum of our cohort. Organ or other structural abnormalities are only rarely reported; in accordance, *LHX2* is predominantly expressed in the nervous system according to the GTEx portal. Liver fibrosis,¹² alopecia,¹¹ or olfactory phenotypes⁵ found in murine models were not observed in any of the individuals described herein. An important role of *LHX2* in nervous system development has been previously suggested.^{6,13,26-28} Conditional knockout mice have an altered position of the hippocampus, probably based on the function of *LHX2* as a suppressor of the hem and antihem (2 secondary organizers) in early embryogenesis.^{13,29} Furthermore, a guidance function for proper formation of the corpus callosum was demonstrated.^{14,28} *Lhx2* knockout in glial cells in the critical development period of the mouse (embryonic days 8.5-10.5) led to complete agenesis of the corpus callosum.²⁸ In our series, dysgenesis of the corpus callosum was observed in 5 individuals.

All but one of the variants with parental genetic information in this study occurred de novo. One individual inherited the variant from a mildly affected mother (I15 and I16). The phenomenon of autosomal-dominant variants being largely de novo and less frequently inherited from a mildly affected or even asymptomatic parent has been increasingly observed.^{23,30} This is especially common for NDDs with nonspecific phenotypes and may be missed with the interpretation of (trio) exome data if the analysis focuses on de novo variants.³¹ In accordance with the increasing awareness for multilocus genomic variation³² and effects on phenotypic delineations,³³ we observed 1 definitive and 1 possible dual diagnosis in our cohort, possibly contributing to a more complex phenotype in these 2 cases.

Another challenge is the interpretation of missense variants. Although LGD variants frequently are classified as pathogenic or likely pathogenic, the relevance of missense variants often remains unclear. This emphasizes the importance of functional assays. However, the accessibility to experimental testing is dependent on the function of the protein and its domains. Of the 7 missense variants identified in this study, 5 were located in either one of the LIM or in the HOX domain. Indeed, we observed reduced binding to the known interaction partner *LDB1*⁸ for the variant located in the first LIM domain (p.(Cys80Ser)). The impaired interaction apparently was not caused by a change in stoichiometry because protein levels of *LHX2* with this variant were similar to the wild type. The *LHX2*-*LDB1* heterotetramer, consisting of an *LHX2* dimer bridged by an *LDB1* dimer via the LIM domains, has been shown to be essential for normal function of *LHX2* as a transcriptional

regulator.^{8,9,34,35} Although we saw less impaired interaction of variant p.(Cys80Ser) when co-expressing wild-type *LHX2* in our in vitro assay, we cannot rule out that this abrogated interaction from p.(Cys80Ser) may affect complex formation in a dominant negative fashion in vivo.

The importance of this interaction mechanism has been previously demonstrated in *Drosophila melanogaster*, in which the interaction of *LDB1* ortholog *CHIP* and *LHX2* ortholog *apterous* was found to be indispensable for the axonal guidance in the ventral nerve cord as well as dorsoventral wing development.^{9,26,34,35} Furthermore, impaired *LDB1*/*LHX2* interaction in mice resulted in a lack of specification in early stages of hippocampus development.⁸ Of note, for p.(Cys146Tyr), the variant located in the second LIM domain, we did not observe any impaired interaction with *LDB1*. One might speculate whether there are subtle differences in specificity of the 2 LIM domains for interaction with *LDB1* and *LHX2* itself, which could possibly explain the observed differences. A slightly weaker interaction that is not detectable in this binding assay may possibly already be functionally relevant in vivo. In line with this, we found impaired transactivation capabilities for both variants located in the LIM domains in the luciferase assay, suggesting that both variants indeed impair *LHX2* function. *LHX2* interacts also with other proteins or complexes, such as the NuRD complex³⁶ and *MSX1*.³⁷ For *MSX1*, this interaction is mediated via the HOX domain,³⁷ whereas the interaction domain is unknown for the NuRD complex. Although physical interaction with *MSX1* or NuRD complex component *LSD1* was not impaired by any of the tested missense variants in vitro, it currently remains elusive whether any of the variants affect NuRD complex or *MSX1* interaction in vivo.

For 2 of the 3 missense variants located in the HOX domain (p.(Asn316Lys) and p.(Arg318Leu)), we observed formation of nucleolar aggregates in vitro. Similar nucleolar aggregates, so called aggresomes, have been previously described as intranuclear detention centers for proteins meant for degradation.^{38,39} Structural modeling indicated that these 2 variants affect a DNA-binding site and thus might indeed compromise normal function and result in aggregation in the nucleolus. In accordance, we found impaired transactivation in the luciferase assay for both variants. The third variant (p.(Lys294Glu)) in the HOX domain did not result in aggregate formation and is not predicted to affect direct DNA binding. However, as has been shown for other HOX domains, one may speculate that this position might be involved in cooperative DNA binding due to interaction with a second HOX domain.¹⁷ We did not observe impaired transactivation for this variant in a luciferase assay. It is possible that this variant may only be involved in transactivation of specific targets that we could not pick up with this assay. This highlights the difficulties to identify suitable functional assays to assess all the potentially diverse effects of missense variants on various protein functions. With these in vitro assays, we are unable to rule out possible dominant negative effects in vivo. However,

lack of transcriptional activation of LHX2 harboring the tested variants and the clinical phenotype of the individuals that is comparable to the other cases with LGD variants still support a loss-of-function mechanism for the missense variants. Of note, as different functional assays were performed in different cell lines, we cannot rule out masking of specific phenotypes in certain assays because of the different cell lines used. In total, we demonstrate a functional consequence for 4 of the 6 missense variants assessed, supporting their pathogenic relevance. In vitro impairment of LHX2 function by missense variants in combination with a phenotype indistinguishable from that associated with LGD variants points to LHX2 loss of function or haploinsufficiency as the underlying mechanism of this NDD.

In conclusion, we establish *LHX2* as an NDD gene by identifying largely de novo missense and LGD variants in 19 individuals from 18 families with a variable ID and/or behavioral anomalies and by confirming a functional consequence of several missense variants.

Data Availability

Variants listed in this paper were submitted to LOVD (accession #00427836-00427852). The data that support the findings of this study are available from the corresponding author upon request.

Acknowledgments

The authors thank all participating individuals and their families.

Funding

A.G. was supported by a Bern Center for Precision Medicine young investigator grant. C.Z. was supported by a grant of the German Research Foundation/Deutsche Forschungsgemeinschaft (DFG, ZW184/6-1). Sequencing and analysis for one of the included cases was performed by the Broad Institute Center for Mendelian Genomics and was funded by the National Human Genome Research Institute, the National Eye Institute, and the National Heart, Lung, and Blood Institute grants UM1 HG008900 and R01 HG009141, and by the Chan Zuckerberg Initiative to the Rare Genomes Project. Work by the Ontario, Canada-based group (Costain, Morel) was performed under the Care4Rare Canada Consortium funded by Genome Canada and the Ontario Genomics Institute (OGI-147), the Canadian Institutes of Health Research, Ontario Research Fund, Genome Alberta, Genome British Columbia, Genome Quebec, Children's Hospital of Eastern Ontario Foundation, and McLaughlin Centre for Molecular Medicine. The Ontario-based authors (G.C., C.F.M.) would like to thank all C4R-SOLVE study staff at the

Children's Hospital of Eastern Ontario Research Institute, Alberta Children's Hospital, the Hospital for Sick Children, and BC Children's Research Institute, for their contribution to the infrastructure of Care4Rare Canada.

Author Information

Conceptualization: A.G., W.K.C., C.Z.; Data Curation: C.M.S., A.G., H.S., W.K.C., C.Z.; Formal Analysis: C.M.S., A.G., H.S.; Investigation: C.M.S., A.G., G.C., C.F.M., L.M., J.S., C.Q., M.F., J.K., R.P., C.J.S., A.S.A.C., G.L., S.S., A.O.-L., R.J.S., J.K.S., D.S., D.E.-F., K.Mor., T.B.P., M.P.N., A.T., B.I., K.Mon., A.R., H.S., W.K.C., C.Z.; Supervision: W.K.C., C.Z.; Visualization: C.M.S., A.G.; Writing-original draft: C.M.S., A.G., W.K.C., C.Z.; Writing-review and editing: G.C., C.F.M., L.M., J.S., C.Q., M.F., J.K., R.P., C.J.S., A.S.A.C., G.L., S.S., A.O.-L., R.J.S., J.K.S., D.S., D.E.-F., K.Mor., T.B.P., M.P.N., A.T., B.I., K.Mon., A.R., H.S.

Ethics Declaration

The study was approved by the cantonal research ethics committee of Bern. Genetic testing in various centers was performed either in a clinical diagnostic setting, or in a research setting, approved by the ethical review board of the respective collaborating institutions (Supplemental Table 1). For publication of genetic and clinical data (as well as publication of affected individuals' photographs), informed consent was obtained from the individuals and their parents or legal guardians.

Conflict of Interest

A.O.-L. is a paid member of the Scientific Advisory Board of SPARK for Autism. M.P.N., K.Mon., and T.B.P. are employees of GeneDx, LLC. All other authors declare no conflicts of interest.

Additional Information

The online version of this article (<https://doi.org/10.1016/j.gim.2023.100839>) contains supplementary material, which is available to authorized users.

Affiliations

¹Department of Human Genetics, Inselspital Bern, University of Bern, Bern, Switzerland; ²Department for Biomedical Research, University of Bern, Bern, Switzerland; ³Bern Center

for Precision Medicine (BCPM), University of Bern, Bern, Switzerland; ⁴Division of Clinical and Metabolic Genetics, The Hospital for Sick Children, Toronto, Ontario, Canada; ⁵Program in Genetics and Genome Biology, The Hospital for Sick Children, Toronto, Ontario, Canada; ⁶Department of Paediatrics, University of Toronto, Toronto, Ontario, Canada; ⁷The Fred A. Litwin Family Centre in Genetic Medicine, University Health Network and Mount Sinai Hospital, Toronto, Ontario, Canada; ⁸Department of Medicine, University of Toronto, Toronto, Ontario, Canada; ⁹Division of Human Genetics, Department of Pediatrics, Warren Alpert Medical School of Brown University, Hasbro Children's Hospital/Rhode Island Hospital, Providence, RI; ¹⁰Clinical Genetics Department, CHU Hôpital Sud, Rennes, France; ¹¹Service de Génétique Moléculaire et Génomique, CHU, Rennes, France; ¹²Univ Rennes, CNRS, IGDR, UMR 6290, Rennes, France; ¹³Division of Genetics, Department of Pediatrics, Nemours/Alfred I. DuPont Hospital for Children, Wilmington, DE; ¹⁴Genomic Medicine Center, Department of Pathology and Laboratory Medicine, Children's Mercy Kansas City, Kansas City, MO; ¹⁵University of Missouri-Kansas City School of Medicine, Kansas City, MO; ¹⁶Broad Center for Mendelian Genomics, Program in Medical and Population Genetics, Broad Institute of MIT and Harvard, Cambridge, MA; ¹⁷Division of Genetics and Genomics, Boston Children's Hospital, Harvard Medical School, Boston, MA; ¹⁸Schneider Children's Medical Center of Israel, Petach Tikvah, Israel; ¹⁹Division of Medical Genetics, Department of Pediatrics, David Geffen School of Medicine, UCLA, Los Angeles, CA; ²⁰Movement Disorders Program, Department of Neurology, Boston Children's Hospital, Harvard Medical School, Boston, MA; ²¹GeneDx, LLC, Gaithersburg, MD; ²²Columbia University Vagelos College of Physicians and Surgeons, New York, NY; ²³Department of Medical Genetics, CHU Nantes, Nantes, France; ²⁴Institute of Human Genetics, Friedrich-Alexander-Universität Erlangen-Nürnberg, Erlangen, Germany; ²⁵Centre for Rare Diseases Erlangen (ZSEER), University Hospital Erlangen, Friedrich-Alexander University of Erlangen-Nürnberg (FAU), Erlangen, Germany; ²⁶Institut für Biochemie, Friedrich-Alexander-Universität Erlangen-Nürnberg, Erlangen, Germany; ²⁷Care4Rare Canada, Ottawa, Ontario, Canada; ²⁸Departments of Pediatrics and Medicine, Columbia University, New York, NY

References

- Kochinke K, Zweier C, Nijhof B, et al. Systematic phenomics analysis deconvolutes genes mutated in intellectual disability into biologically coherent modules. *Am J Hum Genet.* 2016;98(1):149-164. <http://doi.org/10.1016/j.ajhg.2015.11.024>
- Xu Y, Baldassare M, Fisher P, et al. LH-2: a LIM/homeodomain gene expressed in developing lymphocytes and neural cells. *Proc Natl Acad Sci U S A.* 1993;90(1):227-231. <http://doi.org/10.1073/pnas.90.1.227>
- Hou PS, Chuang CY, Kao CF, et al. LHX2 regulates the neural differentiation of human embryonic stem cells via transcriptional modulation of PAX6 and CER1. *Nucleic Acids Res.* 2013;41(16):7753-7770. <http://doi.org/10.1093/nar/gkt567>
- Zibetti C, Liu S, Wan J, Qian J, Blackshaw S. Epigenomic profiling of retinal progenitors reveals LHX2 is required for developmental regulation of open chromatin. *Commun Biol.* 2019;2:142. <http://doi.org/10.1038/s42003-019-0375-9>
- Monahan K, Horta A, Lomvardas S. LHX2- and LDB1-mediated trans interactions regulate olfactory receptor choice. *Nature.* 2019;565(7740):448-453. <http://doi.org/10.1038/s41586-018-0845-0>
- Rincón-Limas DE, Lu CH, Canal I, et al. Conservation of the expression and function of apterous orthologs in *Drosophila* and mammals. *Proc Natl Acad Sci U S A.* 1999;96(5):2165-2170. <http://doi.org/10.1073/pnas.96.5.2165>
- Dawid IB, Toyama R, Taira M. LIM domain proteins. *C R Acad Sci III.* 1995;318(3):295-306.
- Kinare V, Iyer A, Padmanabhan H, et al. An evolutionarily conserved Lhx2-Ldb1 interaction regulates the acquisition of hippocampal cell fate and regional identity. *Development.* 2020;147(20):dev187856. <http://doi.org/10.1242/dev.187856>
- Rincón-Limas DE, Lu CH, Canal I, Botas J. The level of DLDB/CHP controls the activity of the LIM homeodomain protein apterous: evidence for a functional tetramer complex in vivo. *EMBO J.* 2000;19(11):2602-2614. <http://doi.org/10.1093/emboj/19.11.2602>
- Porter FD, Drago J, Xu Y, et al. Lhx2, a LIM homeobox gene, is required for eye, forebrain, and definitive erythrocyte development. *Development.* 1997;124(15):2935-2944. <http://doi.org/10.1242/dev.124.15.2935>
- Folgueras AR, Guo X, Pasolli HA, et al. Architectural niche organization by LHX2 is linked to hair follicle stem cell function. *Cell Stem Cell.* 2013;13(3):314-327. <http://doi.org/10.1016/j.stem.2013.06.018>
- Wandzioch E, Kolterud A, Jacobsson M, Friedman SL, Carlsson L. Lhx2-/- mice develop liver fibrosis. *Proc Natl Acad Sci U S A.* 2004;101(47):16549-16554. <http://doi.org/10.1073/pnas.0404678101>
- Mangale VS, Hirokawa KE, Satyaki PR, et al. Lhx2 selector activity specifies cortical identity and suppresses hippocampal organizer fate. *Science.* 2008;319(5861):304-309. <http://doi.org/10.1126/science.1151695>
- Shu T, Richards LJ. Cortical axon guidance by the glial wedge during the development of the corpus callosum. *J Neurosci.* 2001;21(8):2749-2758. <http://doi.org/10.1523/JNEUROSCI.21-08-02749.2001>
- Sobreira N, Schietecat F, Valle D, Hamosh A. GeneMatcher: a matching tool for connecting investigators with an interest in the same gene. *Hum Mutat.* 2015;36(10):928-930. <http://doi.org/10.1002/humu.22844>
- Gadd MS, Jacques DA, Nisevic I, et al. A structural basis for the regulation of the LIM-homeodomain protein islet 1 (Isl1) by intra- and intermolecular interactions. *J Biol Chem.* 2013;288(30):21924-21935. <http://doi.org/10.1074/jbc.M113.478586>
- Miyazono K, Zhi Y, Takamura Y, et al. Cooperative DNA-binding and sequence-recognition mechanism of aristaless and clawless. *EMBO J.* 2010;29(9):1613-1623. <http://doi.org/10.1038/emboj.2010.53>
- Guex N, Peitsch MC. SWISS-MODEL and the Swiss-PdbViewer: an environment for comparative protein modeling. *Electrophoresis.* 1997;18(15):2714-2723. <http://doi.org/10.1002/elps.1150181505>
- Sayle RA, Milner-White EJ. RASMOL: biomolecular graphics for all. *Trends Biochem Sci.* 1995;20(9):374. [http://doi.org/10.1016/s0968-0004\(00\)89080-5](http://doi.org/10.1016/s0968-0004(00)89080-5)
- Thirunavukkarasu K, Miles RR, Halladay DL, Onyia JE. Cryptic enhancer elements in luciferase reporter vectors respond to the osteoblast-specific transcription factor Osf2/Cbfa1. *BioTechniques.* 2000;28(3):506-510. <http://doi.org/10.2144/00283st09>
- Kaplanis J, Samocha KE, Wiel L, et al. Evidence for 28 genetic disorders discovered by combining healthcare and research data. *Nature.* 2020;586(7831):757-762. <http://doi.org/10.1038/s41586-020-2832-5>
- Richter F, Morton SU, Kim SW, et al. Genomic analyses implicate noncoding de novo variants in congenital heart disease. *Nat Genet.* 2020;52(8):769-777. <http://doi.org/10.1038/s41588-020-0652-z>
- Zhou X, Feliciano P, Shu C, et al. Integrating de novo and inherited variants in 42,607 autism cases identifies mutations in new moderate-risk genes. *Nat Genet.* 2022;54(9):1305-1319. <http://doi.org/10.1038/s41588-022-01148-2>

24. Karczewski KJ, Francioli LC, Tiao G, et al. The mutational constraint spectrum quantified from variation in 141,456 humans. *Nature*. 2020;581(7809):434-443. <http://doi.org/10.1038/s41586-020-2308-7>
25. Lek M, Karczewski KJ, Minikel EV, et al. Analysis of protein-coding genetic variation in 60,706 humans. *Nature*. 2016;536(7616):285-291. <http://doi.org/10.1038/nature19057>
26. van Meyel DJ, O'Keefe DD, Thor S, Jurata LW, Gill GN, Thomas JB. Chip is an essential cofactor for apterous in the regulation of axon guidance in *Drosophila*. *Development*. 2000;127(9):1823-1831. <http://doi.org/10.1242/dev.127.9.1823>
27. Chou SJ, Tole S. Lhx2, an evolutionarily conserved, multifunctional regulator of forebrain development. *Brain Res*. 2019;1705:1-14. <http://doi.org/10.1016/j.brainres.2018.02.046>
28. Chinn GA, Hirokawa KE, Chuang TM, et al. Agenesis of the corpus callosum due to defective glial wedge formation in Lhx2 mutant mice. *Cereb Cortex*. 2015;25(9):2707-2718. <http://doi.org/10.1093/cercor/bhu067>
29. Godbole G, Shetty AS, Roy A, et al. Hierarchical genetic interactions between FOXG1 and LHX2 regulate the formation of the cortical hem in the developing telencephalon. *Development*. 2018;145(1):dev154583. <http://doi.org/10.1242/dev.154583>
30. Konrad EDH, Nardini N, Caliebe A, et al. CTCF variants in 39 individuals with a variable neurodevelopmental disorder broaden the mutational and clinical spectrum. *Genet Med*. 2019;21(12):2723-2733. <http://doi.org/10.1038/s41436-019-0585-z>
31. Popp B, Ekici AB, Thiel CT, et al. Exome Pool-Seq in neurodevelopmental disorders. *Eur J Hum Genet*. 2017;25(12):1364-1376. <http://doi.org/10.1038/s41431-017-0022-1>
32. Posey JE, Rosenfeld JA, James RA, et al. Molecular diagnostic experience of whole-exome sequencing in adult patients. *Genet Med*. 2016;18(7):678-685. <http://doi.org/10.1038/gim.2015.142>
33. Karaca E, Posey JE, Coban Akdemir Z, et al. Phenotypic expansion illuminates multilocus pathogenic variation. *Genet Med*. 2018;20(12):1528-1537. <http://doi.org/10.1038/gim.2018.33>
34. Milán M, Cohen SM. Regulation of LIM homeodomain activity in vivo: a tetramer of dLDB and apterous confers activity and capacity for regulation by dLMO. *Mol Cell*. 1999;4(2):267-273. [http://doi.org/10.1016/s1097-2765\(00\)80374-3](http://doi.org/10.1016/s1097-2765(00)80374-3)
35. van Meyel DJ, O'Keefe DD, Jurata LW, Thor S, Gill GN, Thomas JB. Chip and apterous physically interact to form a functional complex during *Drosophila* development. *Mol Cell*. 1999;4(2):259-265. [http://doi.org/10.1016/s1097-2765\(00\)80373-1](http://doi.org/10.1016/s1097-2765(00)80373-1)
36. Muralidharan B, Khatri Z, Maheshwari U, et al. LHX2 interacts with the NuRD complex and regulates cortical neuron subtype determinants Fezf2 and Sox11. *J Neurosci*. 2017;37(1):194-203. <http://doi.org/10.1523/JNEUROSCI.2836-16.2016>
37. Bendall AJ, Rincón-Limas DE, Botas J, Abate-Shen C. Protein complex formation between Msx1 and Lhx2 homeoproteins is incompatible with DNA binding activity. *Differentiation*. 1998;63(3):151-157. <http://doi.org/10.1046/j.1432-0436.1998.6330151.x>
38. Audas TE, Jacob MD, Lee S. The nucleolar detention pathway: a cellular strategy for regulating molecular networks. *Cell Cycle*. 2012;11(11):2059-2062. <http://doi.org/10.4161/cc.20140>
39. Latonen L. Phase-to-phase with nucleoli – stress responses, protein aggregation and novel roles of RNA. *Front Cell Neurosci*. 2019;13:151. <http://doi.org/10.3389/fncel.2019.00151>